Geomagnetic-Cutoff Distribution Functions for Use in Estimating Detector Response to Neutrinos of Atmospheric Origin

D. J. Cooke

Department of Physics, University of Utah, Salt Lake City, Utah 84112

(Received 9 May 1983)

A procedure has been developed for deriving functions which characterize the effect of geomagnetic cutoffs on the charged primary cosmic rays that give rise to neutrinos arriving in any given direction at specified points on or in the earth. These cutoff distribution functions, for use in atmospheric-neutrino flux calculations, have been determined for eight nucleon-decay–experiment sites, by use of a technique which employs the Stormer cutoff expression, and which assumes collinear motion of neutrino and parent primary.

PACS numbers: 94.30.Wb, 94.40.Kw, 94.40.Te

Some large cosmic-ray detectors, such as those used in nucleon-decay research, have a finite response to neutrinos. It is necessary to be able to calculate the expected background flux of neutrinos incident upon such detectors in order to establish whether the angular distribution of certain classes of events has the characteristics of nucleon decay or of neutrino interactions, a distinction which has important physical and astrophysical implications.

The neutrinos produced in the atmosphere (muon and electron neutrinos associated with muon, pion, and kaon decay) constitute a major part of the background. The rate of production of these neutrinos is related to the intensity of primary cosmic rays incident upon the atmosphere, which in turn depends on the primary-cosmic-ray spectrum, and, as discussed by Gaisser,[1] on the geomagnetic cutoffs pertaining in the given situation.

Let the differential intensity of neutrinos reaching a detector in the presence of the geomagnetic field be $A(R, \theta, \varphi)$, where R is rigidity, and θ and φ are the zenith and azimuth angles of neutrino arrival at the detector. If $B(R, \theta, \varphi)$ is the intensity of neutrinos that would exist in the absence of the field, then the functions A and B can be related as follows:

$$A(R, \theta, \varphi) = B(R, \theta, \varphi)C(R, \theta, \varphi), \quad (1)$$

where $C(R, \theta, \varphi)$ expresses the effect of the geomagnetic cutoffs. This "cutoff distribution function" essentially describes, for a detector in a given location, the fraction of the total solid angle of the detector accessible to neutrinos that are descended from charged primaries of any given rigidity.

In deriving these functions, the cutoffs relating to points over the entire earth's surface have to be taken into account. (Because neutrinos can penetrate the earth, their production in the atmosphere on the distant side of the earth, as well as in the local atmospheric mass, is significant.)

A computer-based procedure has been developed for calculating the functions. It assumes that the detector has an isotropic directional response to neutrinos. The entire 4π sr field of view is divided into a number of equal solid angle zones, where each zone, essentially an annulus, lies between defined upper and lower zenith-angle limits. A separate function is determined for each of the zones. (In the present analysis eight $\pi/2$-sr zones are employed, whose zenith-angle limits are listed in Table I.)

As a first step towards deriving the functions, each solid-angle zone is divided into a large number of smaller elements of equal solid angle.

TABLE I. Zenith-angle extent of the eight solid-angle zones for which cutoff distribution functions have been calculated at each site. (The zenith angles are expressed relative to the detector. Thus the first four zones, encompassing zenith angles within the range 0°–90°, are accessible to the downwards-going neutrino flux. The second four zones, lying within the zenith-angle range 90°–180°, are accessible to the upwards-going neutrino flux.)

Zone	Zenith-angle range (deg)	Weighted mean zenith angle (deg)
1	0.0–41.4	27.7
2	41.4–60.0	51.1
3	60.0–75.0	67.9
4	75.5–90.0	82.8
5	90.0–104.5	97.2
6	104.5–120.0	112.1
7	120.0–138.6	128.9
8	138.6–180.0	152.3

The axial zenith and azimuth angles are computed for each element, and then these angles, together with the specified site position, are processed to determine the location and the angle at which the "line-of-sight" vector intersects the assumed production level in the atmosphere (a height of 20 km above the earth in the reported calculations).

A further set of transformations converts these angles into magnetic coordinates. In this work an inclined, offset, magnetic dipole approximating the 1980 geomagnetic field is assumed (an algorithm for conversion of geographic into offset dipole coordinates is given by Cooke[2]). The magnetic coordinates are then inserted into the Stormer cutoff expression[3,4] to yield an estimate of the directional primary-cosmic-ray cutoff. The appropriately normalized Stormer expression is as follows:

$$R_{c,S} = \frac{59.4\cos^4\lambda}{r^2[1+(1-\cos^3\lambda\sin\theta\sin\varphi)^{1/2}]^2}\ \text{GV},$$

where λ is magnetic latitude, θ is zenith angle, φ is azimuth measured clockwise from magnetic north, and r is the distance from the dipole center (in earth-radius units). This expression gives, for any location and direction in a dipole field, the cutoff value below which cosmic-ray access is unconditionally forbidden.

The cutoff values so derived do not taken into account the nondipole components of the earth's field, penumbral effects, or the earth's cosmic-ray "shadow." For these reasons there are significant disparities between calculated real-field cutoffs and the corresponding Stormer estimates. It is estimated, on the basis of direct comparative calculations, as well as by checks made with use of the published real-field cutoffs on Shea and Smart,[5] that the agreement is within about 40%, in directions where the shadow effect is not present. At zenith angles greater than about 60°, in directions where the shadow effect exists, the Stormer cutoff systematically underestimates the true effective cutoff, and discrepancies of the order of a factor of 2 can be encountered. In spite of these differences it is felt that, in this first approach, the Stormer cutoff values constitute acceptable approximations to the real-field cutoffs.

Having thus a means for quickly estimating the required directional cutoffs, the summing of the effects of the cutoffs over all the solid-angle elements within a zone is carried out by numerical integration, as follows:

$$C(R,\theta_n) = \sum_{\theta_i=\theta_1}^{\theta_2}\sum_{\varphi_j=0}^{2\pi}\sum_{R=R_1}^{R_k}\frac{P_n(R)}{ij},$$

where

$$P_n = \begin{cases} 1, & R > R_c(\theta_i,\varphi_j), \\ 0, & R < R_c(\theta_i,\varphi_j), \end{cases}$$

with $R_c(\theta_i,\varphi_j)$ the cutoff pertaining to the direction θ_i, φ_j.

θ_n refers to the zenith-angle range lying within the nth zone (extending from θ_1 to θ_2). The function C is the same as that in Eq. (1), now integrated over all azimuths. If desired, limited ranges of the parameter φ can be introduced, in which case an azimuth dependence would exist.

The cutoff distribution functions calculated for the sites listed in Table II are presented in Fig. 1. The zenith-angle and latitude dependence of the functions are well displayed in these families

TABLE II. Locations for which cutoff distribution functions have been calculated. A single calculation has been carried out for the two tunnel sites on the French/Italian border because the two experiment locations are sufficiently closely spaced to possess essentially the same cutoff distribution functions.

Country	Location	Geographic coordinates	Magnetic latitude	Vertical cutoff (GV) Stormer	Vertical cutoff (GV) Calculated effective
U.S.A.	Soudan gold mine, Minnesota	48.0 N 268.0 E	56.3 N	1.4	1.0
U.S.A.	Homestake mine, South Dakota	44.5 N 256.4 E	52.2 N	2.1	1.8
U.S.A.	Morton salt mine, Ohio	43.5 N 278.3 E	52.0 N	2.1	1.5
U.S.A.	Silver King mine, Utah	40.6 N 248.5 E	47.6 N	3.1	3.0
France/Italy	Mont Blanc and Frejus tunnels	45.5 N 6.8 E	44.4 N	3.8	5.0
U.S.S.R.	Baksan	43.3 N 42.7 E	36.9 N	6.2	6.0
Japan	Kamioka	36.4 N 137.3 E	27.0 N	10.7	11.2
India	Kolar gold fields	13.0 N 78.4 E	2.2 N	15.9	17.3

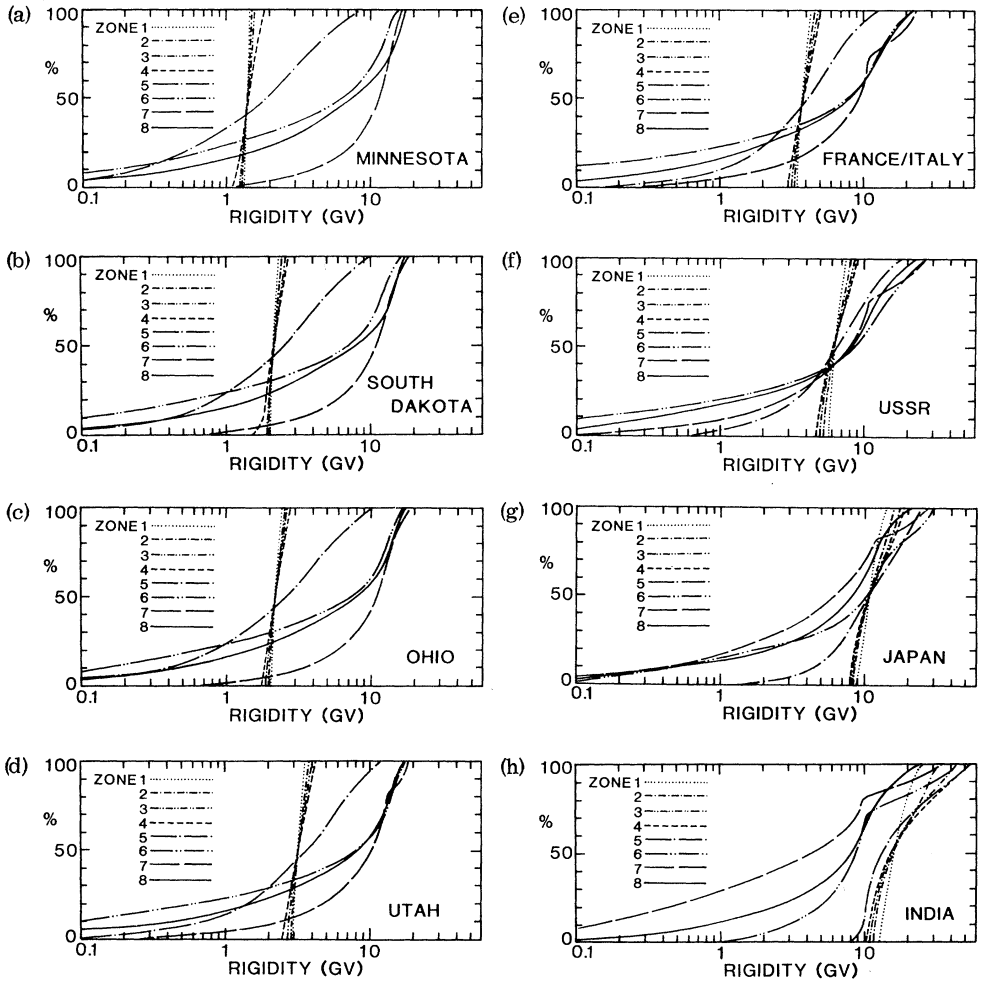

FIG. 1. Integral cutoff distribution functions for the locations shown in Table II. For each location a set of curves is presented, each member of which corresponds to a different solid-angle zone and represents the percentage of the total solid angle of the zone accessible to neutrinos that are descended from charged primaries of any given rigidity. The zenith-angle extent of each zone is identified in Table I.

of curves, which are arranged in order of decreasing magnetic latitude.

It is believed that these functions have basically the correct form, in spite of the simplified approach to the calculations. It is worth noting that any step to improve the precision of the functions by introducing real-field cutoffs, or by taking into account the transverse momentum in the primary-cosmic-ray interactions, would require an amount of computer time greater by many orders of magnitude. That the neutrino events rate observed by the particle detectors are extremely low, in any case, argues for the simpler approach employed at this time.

The effect of the simplifying assumptions on the functions may be anticipated. Because of the nature of the Stormer-cutoff-estimate errors, there might be expected to be a shift in the rigidity position of the functions, in particular for those curves relating to the downward-going neutrino flux. Note, for example, that for zones 1 through 5, the median value of the functions lies at a rigidity value corresponding to the vertical Stormer cutoff value. This fact suggests that, as a first-order correction, these curves could be displaced to positions for which the median value of the functions lies at the real-field vertical effective cutoff pertaining to each individual site. For the upward-going neutrino flux the cutoff errors would probably produce a combined shift in position and broadening in rigidity extent.

If a more realistic, three-dimensional, neutrino production model were to be utilized, a "smearing" of the functions could be expected,

which would probably result in a less well defined zenith-angle dependence. On the other hand, the effect of the earth's shadow, and of secondary-particle deflection over large atmospheric path lengths, could be expected to cause the functions applying to near-horizontal directions to extend to rigidity values appreciably greater than the curves indicate.

Gaisser *et al.*[6] have recently used the cutoff distribution functions (as computed in a form relating to upward- and downward-directed detector response cones of various half-angles) in calculating the flux of atmospheric neutrinos. They have shown that the geomagnetic effect has a very significant effect on the expected up-down ratios of neutrinos of the two flavors, and hence on the interpretation of the experimental data from the large detectors.

This research was carried out under the sponsorship of the U. S. Air Force Geophysics Laboratory (under Contract No. F19628-81-K-0020). Thanks are due to Dr. T. K. Gaisser for suggesting that the problem of deriving the cutoff distribution functions be addressed at this time.

[1]T. K. Gaisser, in *Science Underground—1982*, edited by M. M. Nieto *et al.*, AIP Conference Proceedings No. 96 (American Institute of Physics, New York, 1983).

[2]D. J. Cooke, U. S. Air Force Geophysics Laboratory Report No. AFGL-TR83-0102, 1983 (unpublished).

[3]C. Stormer, Astrophysics 1, 237 (1930).

[4]C. Stormer, *The Polar Aurora* (Oxford Univ. Press, London, 1955).

[5]M. A. Shea and D. F. Smart, U. S. Air Force Geophysics Laboratory Report No. AFGL-TR-82-0320, 1982 (unpublished).

[6]T. K. Gaisser, T. Stanev, S. A. Bludman, and H. Lee, Phys. Rev. Lett. 51, 223 (1983).